Int. Agrophysics, 1995, 9, 67-73

ADSORPTION OF WATER VAPOUR ON MONTMORILLONITE: GRAND CANONICAL ENSEMBLE MONTE CARLO SIMULATIONS

A. Delville[1], *S. Sokołowski*[2], *E. Kozak*[3], *Z. Sokołowska*[3]

[1]Centre de Recherche sur la Matiére Divisée, CNRS, 45071 Orléans Cedex 02, France
[2]HLRZ-KFA Jülich, 5170 Jülich, Germany
[3]Institute of Agrophysics, Polish Academy of Sciences, Doświadczalna 4, 20-236 Lublin, Poland

Accepted August 31, 1994

A b s t r a c t. The Grand Canonical Ensemble Monte Carlo simulation method is applied to study adsorption of water vapour on external and internal surfaces of sodium montmorillonite. The model uses MINDO water-clay and cation-clay potentials and empirical water-water and water-cation potentials. The results of investigations of thermodynamic and structural properties of adsorbed water are reported.

K e y w o r d s: water vapour, montmorillonite, Grand Canonical Ensemble Monte Carlo simulation

INTRODUCTION

In the last few years there has been considerable interest in applications of computer simulations to study the behaviour of water and water solutions at solid interfaces and at the surfaces of clay minerals, in particular [2,5-7,9,19,24]. These sudies require detailed knowledge of the stucture of clay minerals [3]. Moreover, several experimental works concerning the behaviour of the liquid water, as well as adsorption of water vapour on clay minerals make comparisons with experimental results possible [4,8,12,13,15-17,20,21].

In the case of swelling minerals, the adsorption processes of polar substances take place on their external and internal surfaces and the behaviour of water at external surfaces and in pore spaces is different. For example, ellipsometry measurements show clearly non-wetting behaviour of external mica surface [18], while swelling clays of the same charge density wets perfectly [21].

The aim of this work is to present the results of Grand Canonical Ensemble Monte Carlo (GCMC) simulations of adsorption of water on a single clay surface and inside slit-like pores. The model of the clay corresponds to the structure of sodium montmorillonite.

INTERACTION POTENTIALS

Many interaction potentials have been proposed to describe bulk water and the best of these are able to reproduce a wide range of structural and thermodynamic properties of water. One of the most convenient models is the so-called TIP4P model [10]: The water molecule is a rigid unit with the hydrogen-oxygen distance $9.57 \cdot 10^{-2}$ nm and the angle 105.52°. The molecule consists of four interaction sites, two of them are hydrogen atoms, which carry a charge of -0.52 *e*. The third site balances this charge and is placed on the axis at the distance of $1.5 \cdot 10^{-2}$ nm from the oxygen, towards hydrogen atoms. The fourth site is just oxygen. The total energy of a pair of water molecules is the sum of nine Coulombic terms and the van der Waals oxygen-oxygen interactions:

$$u_{oo}^{ww} = A_{oo}/r_{oo}^{12} - B_{oo}/r_{oo}^{6} \qquad (1)$$

with $A_{oo} = 2.511208 \cdot 10^{-6}$ kJ nm^{12} and $B_{oo} = 2.55395 \cdot 10^{-3}$ kJ nm^6.

The model of a single clay surface was identical with that described by Delville [6]. The clay unit $Al_2Si_6O_{24}H_{18}$ is built of a hexagonal cavity of silicates and two octahedral alumina. The model also takes into account substitution of one Si^{IV} atoms by one Al^{III} atom. The substituted unit formula is $Al_3Si_5O_{24}H_{18}^-$ and this substitution introduces negative charges into the network. The single clay sheet used in simulations consists of 24 unit cells. The detailed description of the positions of all nuclei in the unit clay cell, as well as the local charges of the clay atoms are given in ref. [6]. In order to reproduce the experimental substitution ratio [14], two Si atoms are replaced by Al. In addition to the described network, the model also accounts the presence of exchangeable sodium counterions, neutralizing the negative charge of the network [6]. Consequently, the total water-clay potential is the sum of electrostatic contributions between the charges of water, q_i, and the charges of clay, q_j, (cf. Table 2 in ref. [6]):

$$\upsilon_{ij}^{clw} = \frac{\alpha}{4\pi\varepsilon_0} \sum q_i q_j / r_{ij} , \qquad (2)$$

and the van der Waals interactions between all atoms of H_2O molecule and the clay. These atom-atom potentials are:

$$u_{ij}^{clw} = a_{ij}/r_{ij}^2 - b_{ij}/r_{ij}^6 + c_{ij} \exp(-d_{ij} r_{ij}) . \qquad (3)$$

The values of the parameters of Eq. (3) are given in refs [6,7] and the value of α in Eq. (2) was adjusted to be 2.1126.

The interactions of the mobile sodium ions with the clay are calculated as the sum of electrostatic and van der Waals interactions. The former were described by the formula [6]:

$$\upsilon_{Na} = \frac{\alpha_1 q_{Na}}{4\pi\varepsilon_0} \sum q_j / r_{ij} , \qquad (4)$$

where the summation is carried out over all the charges of the clay. The value of the parameter α_1 is 1.2545.

The van der Waals contribution energy of the cation-clay atom potential is:

$$u_j^{ccl} = -a_j/r_j^6 + b_j/r_j^9 + c_j \exp(-d_j r_j) , \qquad (5)$$

with the parameters of Eq. (4) given in refs [6,7]. We add the water-cation potential to the potentials given above. The van der Waals contributions are: the sum of cation-proton repulsive energies and cation oxygen interaction:

$$u_{NaO}^{wc} = A_{NaO} \exp(-b_{NaO} r) - C_{NaO}/r^4 - D_{NaO}/r^6 , \qquad (6)$$

and

$$u_{NaH}^{wc} = A_{NaH} \exp(-b_{NaH} r) . \qquad (7)$$

The parameters of the above equations are A_{NaO}=1.144·10^5 kJ/mol, b_{NaO}=35.455 nm^{-1}, A_{NaH}=8.612·10^3 kJ/mol, b_{NaH}=33.940 nm^{-1}, C_{NaO}=1.820·10^3 kJ/mol, and D_{NaO}=-3.515·10^3 kJ/mol. Only electrostatic interactions between cations have been taken into account. Neglecting the van der Waals energy is justified by rather large separations between cations.

A detailed discussion of the parameters of the potentials describing interactions of water particles and sodium ions with the surface, together with their justification, is given in ref. [6,7]. We only note here that these potentials have been derived from quantum-mechanical MINDO calculations for a single clay sheet.

We use a continuous field approximation in order to incorporate the long-range electrostatic interaction cut by the minimum image method. For this purpose we introduce an external field contributing to the Coulombic energies of water and Na^+ ions. The charges generating this external field have been calculated from Poisson-Boltzmann treatment of the diffuse layer. This standard procedure [11,22,23] assures the convergence of the counterion concentration profile and energy.

SIMULATION METHOD

We studied water adsorption of water vapour on a single clay surface and between two

clay sheets. The sheet dimensions XL and YL were 3.108 nm and 3.588 nm and periodic boundary conditions have been applied in the tangential directions. In the case of adsorption on a single surface, the simulational box was closed by a hard wall, located at the distance of 200 nm. The model pore, however, was built of two symmetric clay sheets separated by a distance of 2 nm. All these distances have been measured from the plane passing through the Si atoms.

Computer simulations were carried out by using GCMC method [1]. Each Monte Carlo step has consisted of an attempt of a motion of one water or Na^+ ion followed by an attempt of creation or anihilation of one water molecule. The first $1.0 \cdot 10^6$ steps were discarded and the final averages were evaluated from at least $1.5 \cdot 10^6$ interactions.

All simulations have been carried out at T=298 K. Simulations were performed for the charge density equal -0.717392 e nm^{-2}. This charge density are neutralized by 8 Na^+ ions associated with a single clay surface.

The configurational part of the chemical potential at the bulk liquid/vapour coexistence point is $\Delta\mu/kT$=-14.076 and the saturated vapour pressure is 3166.15 Pa. Ideal gas approximation was assumed to relate the relative pressure p/p_s and the chemical potential.

RESULTS AND DISCUSSION

Figure 1 displays the adsorption isotherms. In the case of adsorption on a single surface, we see small steps located at the relative pressure equal to about 0.01, but in general the adsorption isotherm for relative pressures up to 0.97 is flat. This is typical for non-wet surfaces. Similar non-wetting behaviour was also found experimentally [18]. In the case of the adsorption in the pore, the adsorption plateau corresponds to the complete pore filling.

Figure 2 gives the energies of the systems. Comparing the results for the porous system with the energies of the open system having the same single plane charge density, we see that the energy of the porous system, i.e., the stabilization energy is about 20 MJ/mol lower.

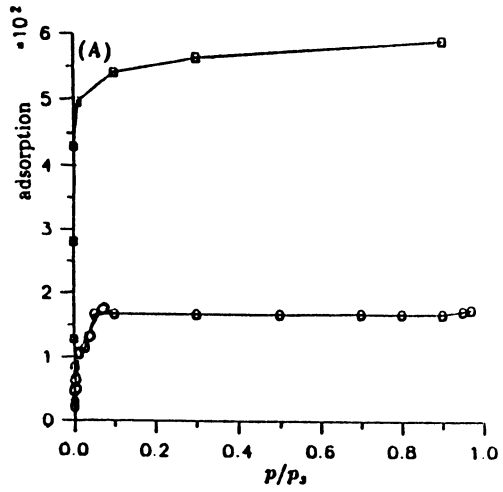

Fig. 1. Adsorption isotherms of water. Squares denote the results obtained for the pore whereas circles are the results for the open surface neutralized by 8 Na^+ counterions.

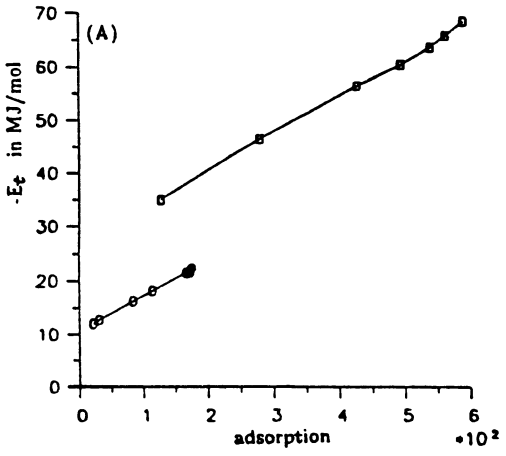

Fig. 2. The total energy plotted as functions of the amount of adsorbed molecules. The meaning of the symbols is the same as in Fig. 1.

Structure of the adsorbed water was investigated evaluating the concentration profiles of oxygen, cation-water radial distribution functions, $g_{NaO}(r)$, as well as by examining the snapshoots of the generated configurations.

Figure 3 presents an example of the snapshoot evaluated at low relative pressure, before the first adsorbed layer is completed.

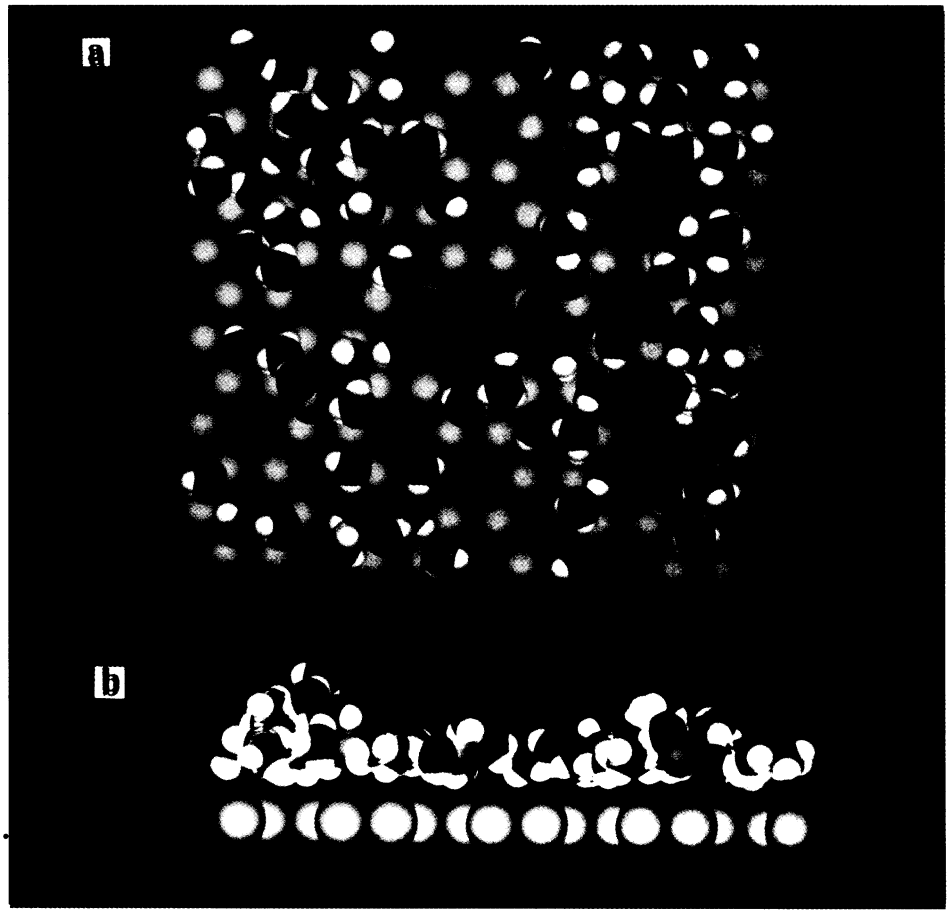

Fig. 3. The snapshoot from the top (a) and lateral (b) view of the adsorbed water molecules. The interface contains 8 Na^+ ions and the relative pressure is 0.00005. Only Si and Al atoms of clay network are displayed.

The number of adsorbed molecules corresponds to the relative surface coverage equal to 1/4. Part B of this figure shows that the adsorbed water forms clusters around cations. Obviously, the swelling ability of dry clay is highly dependent on the chemical nature and accessibility of interlamellar cations [6].

In Fig. 4 we have displayed density profiles evaluated at low relative pressures and for the open system. These density profiles indicate the existence of one well-established adsorbed layer. The filling of this first layer corresponds to the first step in the adsorption isotherm displayed in Fig. 1. The first maximum of the local density is at 0.415 nm from the Si plane and its height is about 100 mol dm^{-3}. This density is two times higher than the liquid water concentration (55.5 mol dm^{-3}). The average distance of sodium cations was found to be greater than the positions of the local density maximum. With an increase of the pressure the first local density peak spreads into complex, short-range structure and its maximum position is slightly shifted towards the surface. Clearly, 8 sodium cations are not enough to enforce development of a thick adsorbed film.

The evaluated mean radial distribution functions of oxygen atoms around cations have been next used to calculate the solvation number of cations - see Fig. 5. The curve for the open

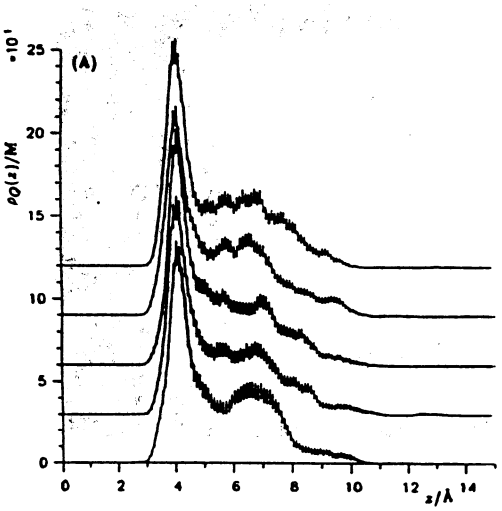

Fig. 4. Oxygen concentration profiles for the single clay surface. The curves (from the bottom) were evaluated for the relative vapour pressures 0.1, 0.3, 0.5, 0.7 and 0.9.

systems exhibits a step. The position of this step is nearly the same as the position of the step in the adsorption isotherm. The coordination number jumps to 6 at higher relative pressures. The coordination number 4 corresponds to planar arrangement of water around cations. Development of the second layer of adsorbed

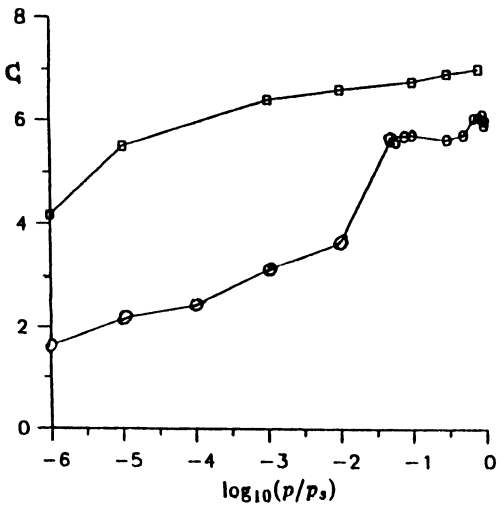

Fig. 5. The dependence of the cation solvation numbers, C, for the investigated systems as a function of the partial pressure. The abbreviations of the systems are the same as in Fig. 1.

water puts two more water molecules into the first coordination shell of the cation.

Summing up, the adsorption of water on the external surface of clay process by step: first complete filling of the first layer, and next building of the second layer. The second layer water molecules are directly connected to the cations.

Let us now discuss structure of water adsorbed inside the pore. Figure 6 shows an example of snapshoot of the water molecules adsorbed in the pore at the partial pressure $1 \cdot 10^{-5}$. The first layer adjacent to the pore wall is still undersaturated and the water molecules form cluster around cations. This explains why the adsorption in the pore is not a sum of the effects occurring on separate walls.

The average distance of Na^+ ions from the closest pore wall is greater than in the case of the open system and increases with an increase of the relative pressure, but the maximum distance of sodium ions does never excess 0.85 nm.

Figure 7 shows some oxygen profiles in the pore. The locations of the local density maxima are very similar to those observed for the open systems. At the lowest relative pressure ($p/p_s = 10^{-6}$) the first density peak is at 0.42 nm from the wall but when the relative pressure increases, this peak is shifted towards the wall and at p/p_s=0.8 its position is at 0.395 nm. We can see that even at extremely low relative pressure $1 \cdot 10^{-6}$ there are some inner water molecules, although the first layers are far from being completed. The peaks corresponding to the formation of the second layers are seen at the relative pressure $1 \cdot 10^{-5}$. The third layer peak develops at the relative pressure 0.3. We should stress that no signal of capillary condensation phenomenon was observed and the adsorption of water in the pore is a continuous process. The inner water molecules are connected to the water molecules from the first layer.

CONCLUSIONS

We have performed simulations of adsorption of water on single montmorillonite

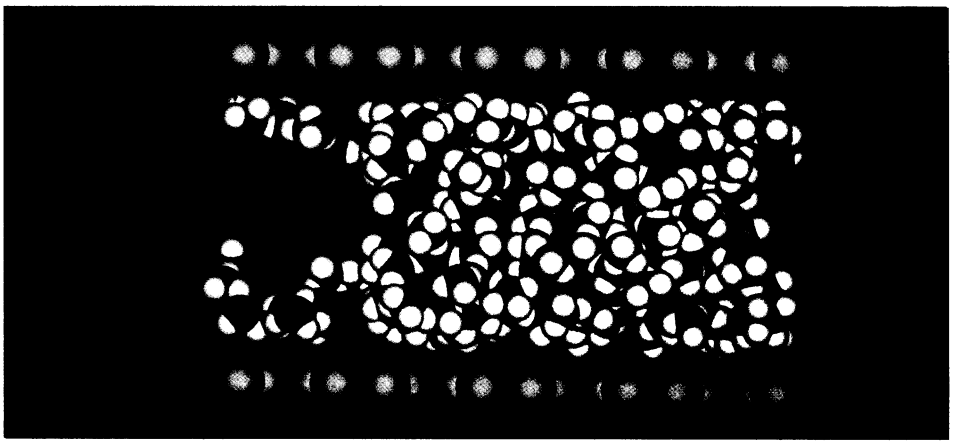

Fig. 6. The views of the evaluated configuration of water molecules inside the pore.

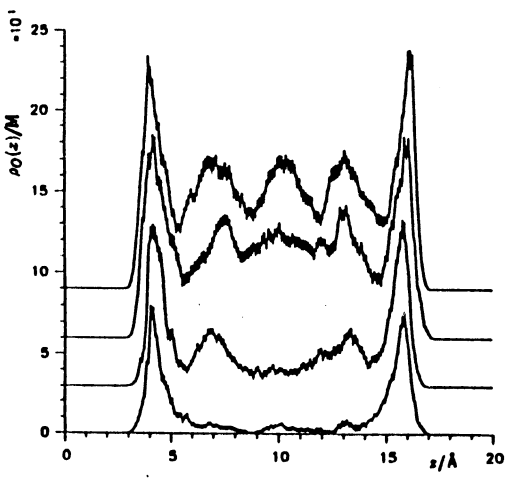

Fig. 7. Concentration profiles of oxygen inside the pore. The subsequent (from the bottom) curves were obtained for the relative pressures 10^{-6}, 10^{-5}, 0.1 and 0.8.

surfaces and between two clay sheets. The results indicate that in the case of adsorption on external surfaces adsorption isotherms show typical non-wetting behaviour. The results demonstrate the differences between adsorption on a single surface and inside the pore. In the latter case the adsorption isotherm is smooth. The filling of the inner part of the pore starts before saturation of the first layer. In the former case, however, the adsorption isotherm shows small step, connected with the filling of the first layer.

REFERENCES

1. **Adams D.J.:** Computer simulations in Grand Canonical Ensemble. Molec. Phys., 28, 1241-1246, 1974.
2. **Aloisi G., Foresti M.L., Guidelli R., Barnes P.:** A Monte Carlo simulation of water molecules near a charged wall. J. Chem. Phys., 91, 5592-5596, 1989.
3. **Brindley G.W., Brown G.:** Crystal Structures of Clay Minerals and Their X-ray Identification. Min. Soc., London, England, 1980.
4. **Cases J., Francois M.:** Etudes des thermodynamiques de l'eau au voisinage des interfaces. Agron., 2, 931-938, 1982.
5. **Christou N.I., Whitehouse J.S., Nicholson D., Parsonage N.G.:** A Monte Carlo study of fluid water in contact with structureless walls. J. Chem. Soc. Faraday Trans., 78, 139-149, 1982.
6. **Delville A.:** Modelling the clay-water interface. Langmuir, 7, 547-555, 1991.
7. **Delville A., Sokołowski S.:** Adsorption of vapor at a solid surface: a molecular model of clay wetting. J. Phys. Chem., 97, 6261-6271, 1993.
8. **Fripiat J., Cases J., Francois M., Letellier M.:** Thermodynamic and microdynamic behavior of water in clay suspensions and gels. J. Colloid Interface Sci., 89, 378-400, 1982.
9. **Grim R.E.:** Chemistry of Clays and Clay Minerals. Mineralogical Society, London, England, 1987.
10. **Jorgensen W.L., Chandrasekhar J., Madura J.D., Impey R.W., Klein M.L.:** Comparison of simple potential functions for simulating liquid water. J. Chem. Phys., 79, 926-935, 1983.
11. **Jönsson B., Wennerström H., Halle B.:** Ion distributions in lamellar liquid crystals. A comparison between results from Monte Carlo simulations and solutions of the Poisson-Boltzmann equation. J. Phys. Chem., 84, 2179-2185, 1980.
12. **Jurinak J.J.:** The effect of pretreatment on the adsorption and desorption of water vapour by lithium

and calcium kaolinite. J. Chem. Phys., 65, 162-164, 1961.

13. **Keren R., Shainberg I.:** Water vapour isotherms and heats of immersion of Na/Ca montmorillonite system. II. Mixed systems. Clays Clay Miner., 27, 145-151, 1979.
14. **Low P.F.:** The swelling of clay: II. Montmorillonites. Soil Sci. Soc. Am. J., 44, 667-676, 1980.
15. **Mikhail R.S., Guindy N.M., Hanafi S.:** Water adsorption on expanding and nonexpanding clay minerals. J. Colloid Interface Sci., 70, 282-292, 1979.
16. **Oliphant J.L., Low P.F.:** The relative partial specific enthalpy of water in montmorillonite-water systems and its relation to the swelling of these systems. J. Colloid Interface Sci., 89, 366-373, 1982.
17. **Orchiston H.D.:** Adsorption of water vapour. II. Clays at 25 °C. Soil Sci., 78, 463-480, 1954.
18. **Radlinska E.Z., Christenson H.K., Ninham B.W.:** Wettability of mica surface by water. In: Proc. 1st Liquid Matter Conference (Ed. K. Bethge). Vol. 14C, Lyon, 1990.
19. **Raghavan K., Foster K., Motakabbir K., Berkowitz M.:** Structure and dynamics of water at Pt(111) interface: Molecular dynamics study. J. Chem. Phys., 94, 2110-2117, 1991.
20. **Sokołowska Z.:** On the role of energetic and geometric heterogeneity in sorption of water vapour by soils. Geoderma, 45, 251-265, 1989.
21. **Taraschevich J.I., Ovscharenko F.D.:** Adsorption on Clay Minerals. Naukova Dumka, Kiev, 1975 (in Russian).
22. **Torrie G.M., Valleau J.P.:** Electric double layers. I. Monte Carlo study of a uniformly charged surface. J. Chem. Phys., 73, 5807-5816, 1980.
23. **Van Megen W., Snook I.J.:** The Grand Canonical Ensemble Monte Carlo method applied to the electrical double layer. J. Chem. Phys., 73, 4656-4662, 1980.
24. **Zhu S.B., Robinson G.W.:** Structure and dynamics of liquid water between plates. J. Chem. Phys., 94, 1403-1410, 1991.